Analysis of the flow rate through rotating shafts in lubricating circuits

23rd Australasian Fluid Mechanics Conference – 23AFMC
Sydney, Australia
4-8 December 2022
Paper No: AFMC2022-24

Analysis of the flow rate through rotating shafts in lubricating circuits

Paola Fresia[1] and Massimo Rundo[1*]

[1]Department of Energy, Politecnico di Torino, Turin, 10129, Italy

* Email: massimo.rundo@polito.it

Abstract

The paper presents the CFD simulation of the oil flow distribution in a rotating system. The aim of the study is to validate the modelling approach for applications in dimensioning and analysing lubrication circuits. A specific experimental assembly was manufactured for measuring the flow rate distribution in a rotating shaft enclosed in a liner with axial inlet and three radial outlets. The flow rate of each outlet was measured by a dedicated turbine flow meter. It was found that, except for high fluid viscosities, the flow rate through the farthest outlet is the highest, due to the inertia of the oil that tends to flow straight on until the last outlet, despite the longest distance, instead of leaving the axial channel through the first radial holes. The angular speed has a slight effect in increasing the nonuniform flow distribution and a significant influence in decreasing the feed pressure. It has been demonstrated that the simulated results are reliable, and the methodology can be used for designing properly the circuit layout in order to obtain a homogeneous flow distribution.

1. Introduction

In different types of machines, the relative motion of the mechanical components at high speed and under significant contact forces needs a proper lubrication. The most important aims of the lubricant flow rate are reduction of the friction and removal of the heat. Regardless of the system, the oil is supplied by a positive displacement pump and distributed by ducts and cooling jets up to the parts to lubricate, such as journal bearings or clutches. Typically, all these components are fed in parallel by a main gallery and their distance from the circuit inlet can be very different. The consequence is that the flow rate distribution is not homogeneous, and it is highly dependent on the layout and on the operating conditions. The risk is that in some points of the circuit the lubrication could be insufficient with a resulting failure of the machine. Since the oil can also flow through passageways drilled directly in rotating shafts, the pressure and velocity field are also affected by the angular speed and this aspect must be considered in the simulation model.

In this context, the design of the circuit layout must be grounded on reliable outcomes of a simulation tool able to reproduce correctly the local pressure drops and the forces generated in a non-inertial reference frame. The lumped parameter approach has the drawback that the pressure loss coefficients are known a priori only for simple geometries and with the hypothesis of a high distance among consecutive resistances. The CFD approach, even if with higher computational times, allows studying complex geometries.

About the simulation of the flow through fixed geometry layouts, such as hydraulic manifolds, a review of the methodologies is presented in (Wang 2011), while a comparison between semi-empirical and CFD approaches for the evaluation of the pressure drops is reported in (Zardin *et al.* 2015). A study of the flow in a high-speed rotating shaft with radial inlet is shown in (Xiong 2015), where the influence of the supply pressure and the angular speed is reported. The effect of the shaft speed up to 2500 rpm on the oil distribution between two groups of radial outlets at different distances from the inlet is reported in (Sharma *et al.* 2022). As far as the study of complex systems with rotating

shafts is concerned, a simulation of the flow rate in a continuous variable speed hydrostatic transmission with multiple radial outlet ports is analysed in the references (Marani *et al*. 2014) and (Ferrari *et al*. 2015). A comprehensive CFD simulation of the entire lubrication system of an internal combustion engine is reported in (Dhar *et al*. 2016).

However, to the best knowledge of the authors, a little attention has been paid on the experimental validation of the flow distribution in a multiple outlet rotating system. In this paper, the outcomes from the simulation of a device with three couples of outlet holes drilled in a shaft rotating up to 5000 rpm are compared to the experimental data. Aim of the study is to find the optimal setting of the CFD model to simulate the flow rate distribution and the inlet pressure, so that the methodology could be used with a high degree of confidence for the simulation of different lubricating circuits with fixed and rotating components.

2. Experimental facility

Since the experimental measurement of the flow rate distribution in a real lubricating circuit is not feasible, for the validation of the simulation approach a specific assembly was designed and manufactured. A cross section is shown in Figure 1. It is made up by a shaft with an axial channel and three couples of radial ducts located at different distances from the oil inlet. The shaft is supported by ball bearings and the right end is provided with a rotary seal. The opposite end of the shaft is used for the connection to a variable speed electric motor of a test rig for positive displacement pumps. Thanks to the elastic rings mounted on the shaft, each couple of holes has an independent outlet port on the housing, so that it is possible to measure separately their flow contribution.

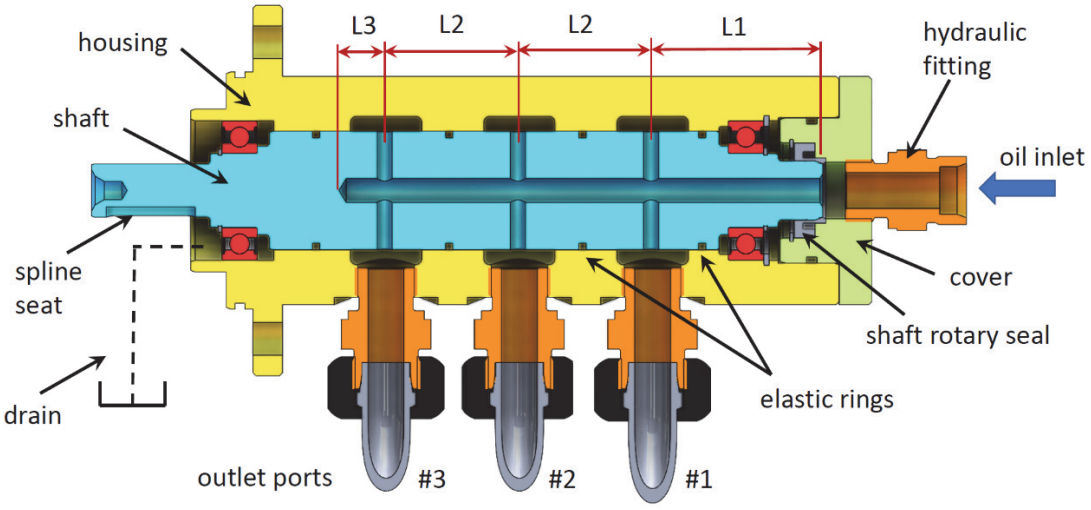

Figure 1. Section view of the rotating device.

For the specific application, the assembly was mounted on the interface block in place of the pump to be tested and was fed by an external hydraulic power unit. The inlet flow rate was controlled by a proportional load sensing directional control valve Danfoss PVG32 and measured by a gear flow meter VSE 1 GPO12V with measuring range 0.05 ÷ 80 L/min and accuracy 0.3% of the measured value. The inlet pressure was measured by a pressure gauge with range -1 ÷ +1.5 relative bar and resolution 0.05 bar. Three identical turbine flow meters KEM Küppers HM 11E with range 6 ÷ 60 L/min were used for measuring the flow rate at the outlet ports. The variation of the constant of proportionality between the volumetric flow rate and the frequency (K factor) was considered by interpolating with a sixth order polynomial the calibration points supplied by the manufacturer at the viscosity used for the tests.

First attempts were made with only two turbine flow meters, since the remaining outlet flow rate could have been measured by difference knowing the inlet flow rate. However, it was found that the lower resistance of the outlet line without the flow meter had a non-negligible effect on the flow rate distribution. Therefore, the same identical geometry, including the same type of hydraulic fittings,

was used for building the circuit downstream from the rotating assembly. The main geometric parameters are reported in Table 1, while a photo of the test rig is shown in Figure 2. The return lines were constituted by three rubber hoses directly connected to the reservoir at atmospheric pressure. A small drain flow due to the leakage in the last elastic ring was collected in a tray located underneath the interface block. The leakage flow, measured by means of a graduated burette, was 8 cm^3/min, value three orders of magnitude smaller with respect to the inlet flow rate; for this reason, the leakage flow across the elastic rings was neglected in the CFD model.

Quantity	Value	Quantity	Value
Shaft outer diameter	40 mm	Length L1	58 mm
Axial channel diameter	8 mm	Length L2	45 mm
Radial ducts' diameter	5 mm	Length L3	13 mm

Table 1. Characteristic dimensions of the experimental assembly.

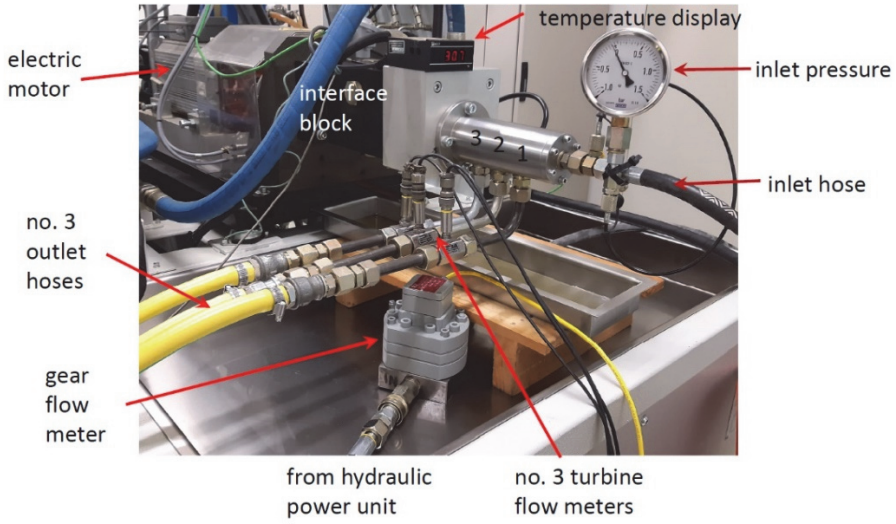

Figure 2. Photo of the test rig.

An ISO VG46 Mobil DTE 25 mineral oil was used as working fluid. The temperature in the reservoir of the hydraulic power unit was maintained constant at 40 °C ± 2 °C by means of a water-oil heat exchanger and of a thermostatic valve. The oil viscosity at 40 °C was checked with a Brookfield AMETEK DV1 viscosimeter, while the density with a Mohr-Westphal balance.

3. CFD model

The CFD model has been developed in ANSYS Fluent® 2021 R1, which discretises the governing equations with the finite volume method. The fluid volume was imported as a step file subdivided in regions: inlet, axial channel with radial holes, and the three volumes of the outlet pipes located upstream of the turbine flow meters. The subdivision helped for the definition of different values of grid density. The ANSYS meshing tool was then used to generate the tetrahedral mesh. For every region, a *body sizing* was utilized defining the elements' dimension and then refinements were applied in the connection areas and along the radial holes of the main axial channel. Inflation layers were also added with the *program controlled* automatic feature in order to correctly solve the boundary layer.

For the CFD analysis a RANS approach was used. The turbulence of the flux was considered with the RNG k-ε model, which permits to simulate flows with low-Reynolds numbers (ANSYS, Inc. 2021). The *Enhance Wall Treatment* was adopted as near-wall modelling, which allows a consistent mesh refinement without a deterioration of the results (ANSYS, Inc. 2021).

All simulations were performed in steady-state conditions. The mass flow rate at the inlet and the atmospheric pressure at the outlets were imposed as boundary conditions. The rotation of the shaft and thus of the axial and radial channels was simulated with the *Multiple Reference Frame* model

(MRF). With this approach the mesh remains fixed, since the relative motion of a rotating zone with respect to adjacent regions is not considered. It is a steady-state approximation where different rotational speeds can be assigned to individual computational volumes. It is equivalent to freeze the rotation of the shaft and to study the flow field at a specific angle. However, several simulations were performed in static conditions with different relative positions between radial channels and outlets, showing no appreciable influence on the calculated flows, so the approximation introduced by the MRF model had no consequences on the outcomes of simulations. These results were then confirmed by experimental tests, in which the shaft was manually positioned at different angles: no differences between measured flows in dissimilar positions were noted.

The pressure-based coupled algorithm was used to solve the coupled system of equations containing the momentum equations and the pressure-based continuity equation, so as to speed-up convergence. The gradients were evaluated using the Green–Gauss node-based method, which is usually recommended for tetrahedral meshes. The 2nd order discretization scheme was used for the pressure equation, the 2nd order upwind for the momentum, turbulent kinetic energy and turbulent dissipation rate equations. The Pseudo-transient method was enabled when simulating rotating conditions, in order to help and speed-up convergence.

A grid independence study was performed in order to find the best compromise between computational time and accuracy: the mass flow rates at the outlets and the inlet pressure were used as observed variables. In particular, the operating condition at 35 L/min inlet flow and 4000 rpm was chosen for this analysis. Figure 3a reports the influence of the number of cells on the calculated outlet flows, while in Figure 3b the effects on the inlet pressure and the computational time. As visible, grid independent results can be obtained with a mesh of 2.7 ca. million cells. The simulations were executed on an eight-core i7-9800X CPU at 3.8 GHz. The final computational mesh, coloured in function of the orthogonal quality of the elements, is shown in Figure 4.

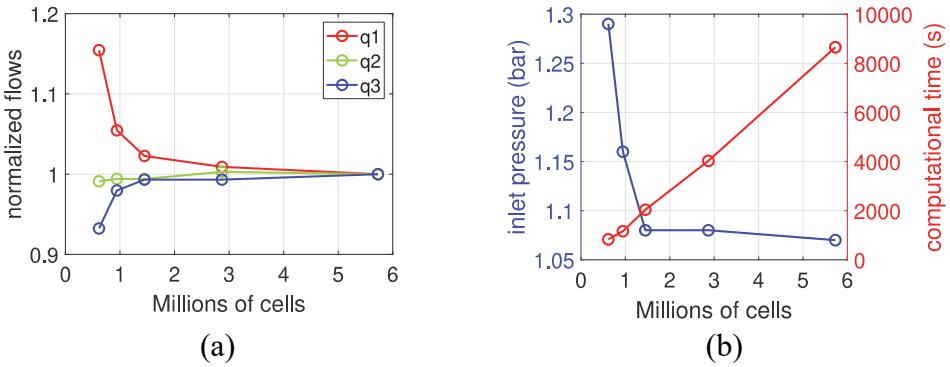

Figure 3. (a) normalized flow rates through the three outlets and (b) inlet pressure and computational time as function on the number of cells.

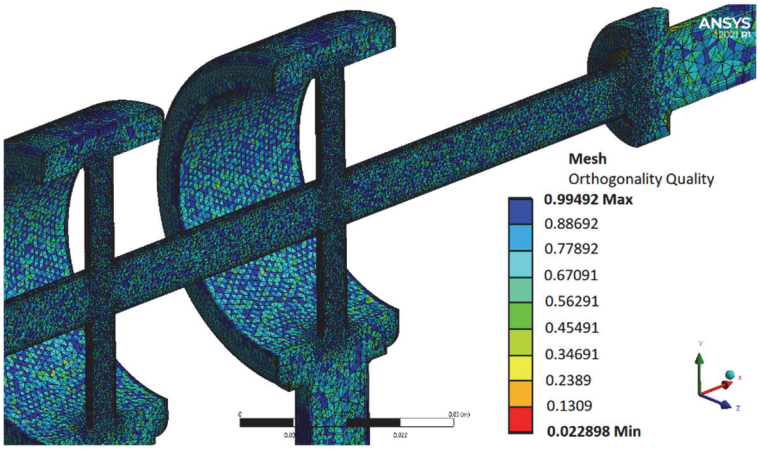

Figure 4. Detail of the mesh with indication of the quality.

4. Results and discussion

For the experimental tests the frequency signals of the flow meters and of the encoder mounted on the shaft were acquired with a NI data acquisition card and managed by a customized Virtual Instrument in Labview®. Once reached the thermal steady state conditions, for all signals the average of six values acquired over a time of 10 s each was calculated. In figure 5 the flow rate distribution through the three outlets is shown for two different inlet flow rates with shaft still and rotating at 5000 rpm. Overall, a good agreement was found between the simulated and experimental results with a maximum discrepancy for the percentage of the row 3 at 15 L/min and 0 rpm (41.6 % simulated against 37.2% experimental).

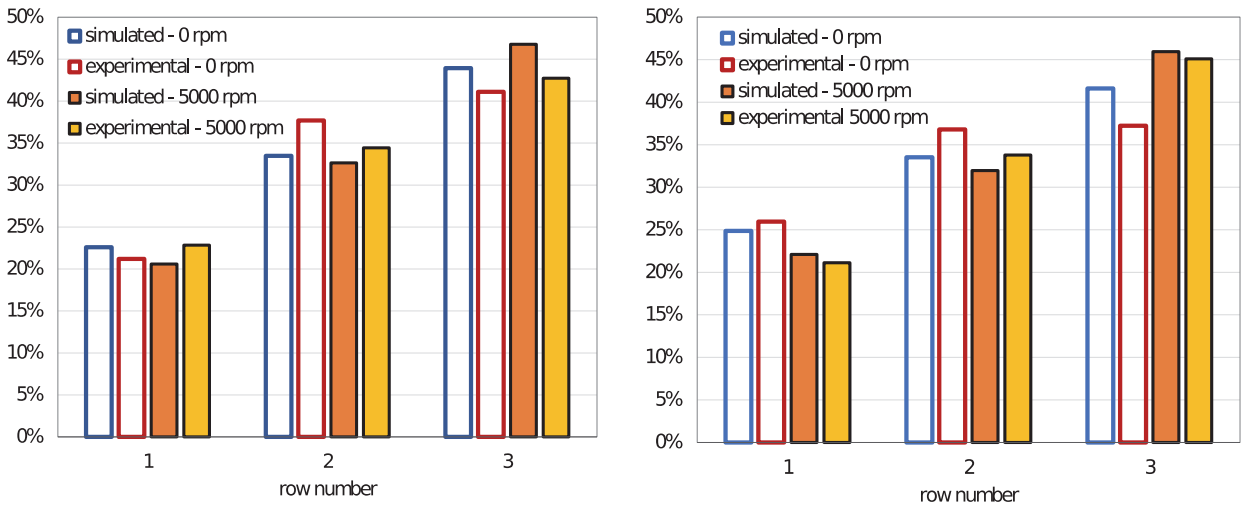

Figure 5. Validation of flow distribution at 0 rpm and 5000 rpm with inlet flow rate of 35 L/min (a) and 15 L/min (b).

It is evident that both the experimental and the simulated trends indicate a significant increment of the flow rate as the distance from the inlet increases, so that with 35 L/min the flow rate through the last row of holes is double with respect to the first. The reason is the inertia of the flow and the negligible pressure drop due to the friction in the axial channel. This statement is confirmed by the fact that a slightly more homogenous distribution is obtained with a smaller inlet flow rate, i.e. with a lower inlet fluid velocity, where a higher flow through the row 1 and a smaller flow through the row 3 is observed with respect to the test at 35 L/min with stationary shaft.

In Figure 6 the fluid velocity is shown. It is evident that the vena contracta coefficient is smaller in the first row and progressively increases in the second and third row.

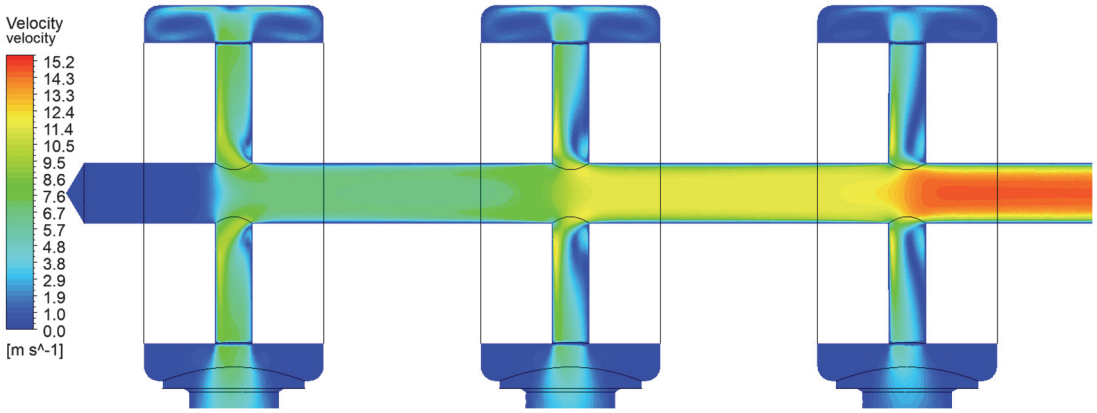

Figure 6. Simulated fluid velocity distribution in correspondence of the intersection between the axial channel and the radial ducts at 35 L/min and 0 rpm.

The different fluid velocities at the inlet of the radial ducts can be appreciated in the Figure 7, where the cross sections along the axis of the rows 1 and 3 are shown. The figure also shows the effect of the shaft rotation on the velocity field that is correctly simulated by the MRF approach.

The shaft speed has an almost negligible influence on the flow distribution with high flow rate, while with 15 L/min the effect is more appreciable; in particular the speed increases the non-uniformity of the distribution, with a higher flow rate through row 3 and a lower through row 1. The reason is because with a lower inlet velocity the fluid is more affected by the suction effect of the centrifugal force generated by the shaft rotation.

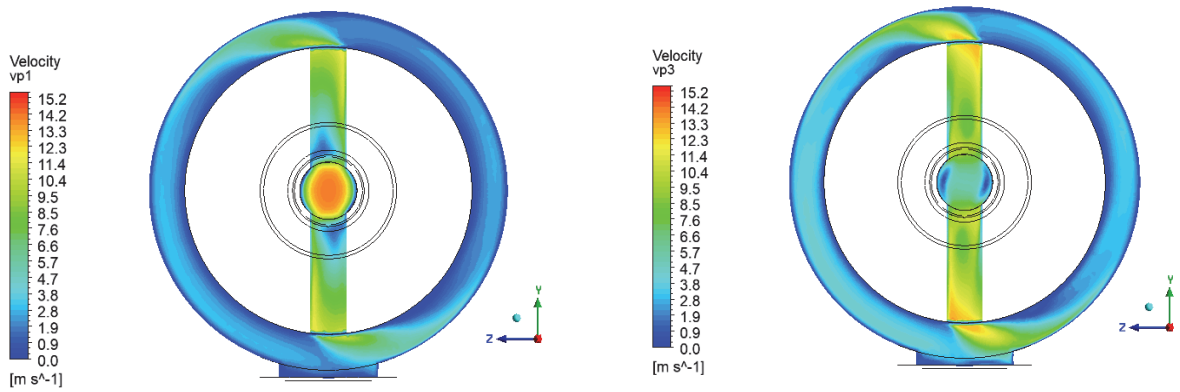

(a) (b)

Figure 7. Simulated fluid velocity distribution in correspondence of the axis of row 1 (a) and row 3 (b) at 35 L/min and 5000 rpm.

The fluid viscosity has a significant effect on the flow distribution. The simulations were repeated at different temperatures using the parameters listed in Table 2. Called ν_{40} the kinematic viscosity at the reference temperature of 40 °C and ν_T at a different temperature, the results as function of the ratio ν_T/ν_{40} are shown in Figure 8. It is evident that the increment of the viscosity increases the dissipation of the kinetic energy in the axial channel. The consequence is a reduction of the flow rate through the last row to the advantage of the first row. Even in this case the effect of the angular speed is negligible.

Fluid temperature (°C)	Dynamic viscosity (Pa·s)	Density (kg/m^3)
0	0.372	884
40	0.0423	859
100	0.0055	822

Table 2. Fluid properties as function of the temperature.

On the contrary, the angular speed has a significant effect on the inlet pressure. Figure 9 presents the dimensionless pressure reduction defined as:

$$\Pi = \frac{p_\omega - p_0}{p_0}, \tag{1}$$

being p_0 the simulated absolute inlet pressure with stationary shaft and p_ω the absolute pressure at a generic angular speed ω. The dimensionless pressure Π ranges between 0 and -1, where the latter limit indicates that the zero absolute pressure has been reached.

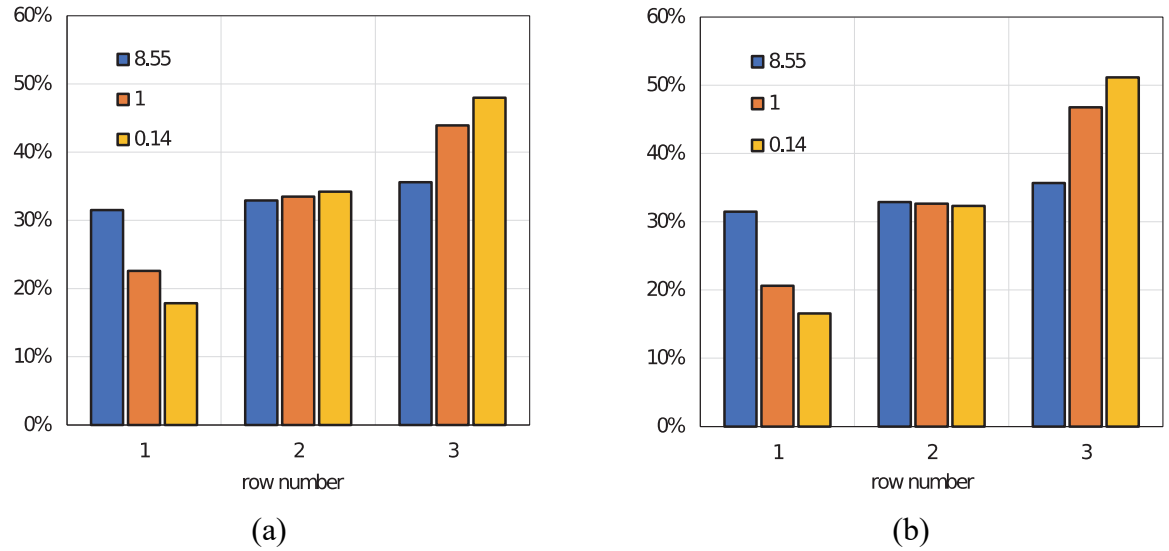

Figure 8. Flow distribution with three different viscosity ratios, inlet flow rate of 35 L/min at 0 rpm (a) and 5000 rpm (b).

The experimental inlet pressure with shaft still was 0.9 relative bar at 35 L/min and 0.3 relative bar at 15 L/min. A fair comparison between the absolute experimental and simulated pressure is not possible, since in the CFD model the turbine flow meters and the remaining part of the circuit downstream of them up to the reservoir have not been simulated. The pressure reduction is induced by the centrifugal force in the radial ducts proportional to the square of the angular speed; the consequence is a suction effect that helps the oil to flow in the circuit. Almost identical results were obtained at 15 L/min, hence the pressure reduction is not affected by the inlet pressure but only by the angular speed.

Since the lubricating circuits work with a typical pressure of a few bar, the reduction shown in Figure 9 is significant and it can lead, depending on the operating conditions and the circuit layout, to negative relative pressures in the axial channel with possible gaseous cavitation (release of dissolved air). For instance, the simulation of an operating condition at 10000 rpm has led to a very low value of the dimensionless pressure variation equal -0.81 (absolute pressure 0.44 bar), it means that at such a speed it could be necessary to throttle the radial ducts in order to keep the pressure above the atmospheric value in the entire circuit.

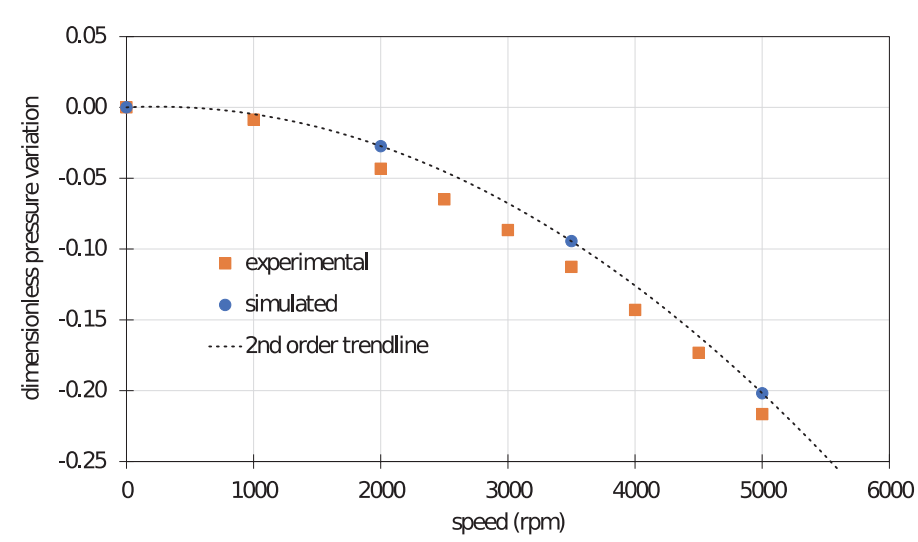

Figure 9. Dimensionless pressure variation at the inlet port as function of the angular speed with flow rate of 35 L/min at 40 °C.

5. Conclusions

The flow in a rotating shaft with three radial outlets has been studied. The developed CFD model is able to correctly reproduce how the inlet flow is distributed. It was found that, contrary to the common sense, for the specific analysed geometry the flow rate increases with the distance from the inlet, hence for balancing the flow distribution it is necessary to increase the resistance through the last holes, i.e. with a smaller diameter. The degree of imbalance increases with the reduction of the fluid viscosity. The angular speed contributes to slightly make less homogeneous the flow distribution. On the contrary, a significant effect was observed on the inlet pressure, with a lowering proportional to the square root of the speed.

This study represents a first step for a more general analysis of the circuit layout and of the fluid parameters affecting the flow distribution. Next steps are the use of the simulation model for determining the influence of geometrical parameters, such as the length and diameter of the internal ducts. The aim is to have a reliable simulation approach to be used in dimensioning complex circuits where the measurement of the flow rate distribution is not possible due to physical constraints.

References

ANSYS, Inc., 2021, Ansys Fluent Theory and User's Guide, Release 2021 R1.

Dhar, S., Afjeh, H., Srinivasan, C., Ranganathan, R. & Jiang, Y. 2016, Transient, Three Dimensional CFD Model of the Complete Engine Lubrication System, *SAE Int. J. Engines* **9**(3):1854-1862.

Ferrari, C., Marani, P. & Ghorpade, K. 2015, CFD Modeling of Lubrication System in Agricultural Power Split Transmission, *13th European Conference of the International Society for Terrain Vehicle Systems*, Oct. 21-23, Rome, Italy.

Marani, P., Ferrari, C., Paoluzzi, R. & Stefano, C. 2014, Methods of Computational Fluid Dynamics for a CVT Transmission Lubrication System of Agricultural Tractor, *9th International Fluid Power Conference*, Mar. 24-26, Aachen, Germany.

Sharma, R., Kumar Gupta, V., Khaware, A. & Kamat, V. 2022, Efficient CFD Methodology for Optimal Design of Oil Cooled Electric Motor Shaft, *7th World Congress on Momentum, Heat and Mass Transfer*, Apr. 7-9, Virtual Conference.

Xiong, Z., Wu, W., Yuan, S. & Hu, J. 2015, Investigation of the Flow Field inside an Oil Distribution Mechanism at High Speed, *2015 International Conference on Fluid Power and Mechatronics*, Aug. 5-7, Harbin, China.

Wang, J. 2011, Theory of flow distribution in manifolds, *Chemical Engineering Journal* **168**:1331-1345.

Zardin, B., Cillo, G., Rinaldini, C.A., Mattarelli, E. & Borghi, M. 2017, Pressure Losses in Hydraulic Manifolds, *Energies* **10**, 310.